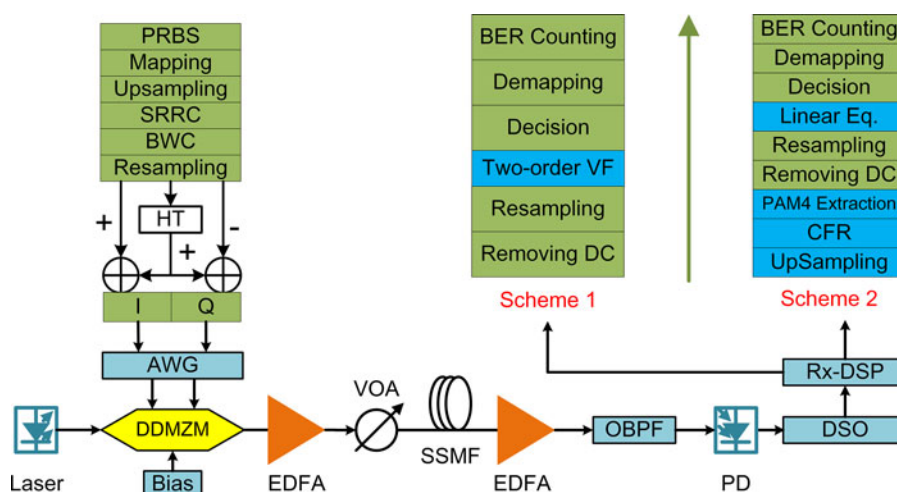


Single-Lane 112-Gbit/s SSB-PAM4 Transmission With Dual-Drive MZM and Kramers–Kronig Detection Over 80-km SSMF

Volume 9, Number 6, December 2017

Liang Shu
Jianqiang Li, *Senior Member, IEEE*
Zhiquan Wan
Fan Gao
Songnian Fu
Xiang Li
Qi Yang
Kun Xu, *Member, IEEE*



DOI: 10.1109/JPHOT.2017.2771221

1943-0655 © 2017 IEEE

Single-Lane 112-Gbit/s SSB-PAM4 Transmission With Dual-Drive MZM and Kramers–Kronig Detection Over 80-km SSMF

Liang Shu¹, Jianqiang Li¹, *Senior Member, IEEE*,
Zhiquan Wan¹, Fan Gao², Songnian Fu², Xiang Li³, Qi Yang³,
and Kun Xu¹, *Member, IEEE*

¹State Key Laboratory of Information Photonics and Optical Communications, Beijing University of Posts and Telecommunications, Beijing 100876, China

²Next Generation Internet Access National Engineering Laboratory, School of Optical and Electronic Information, Huazhong University of Science and Technology, Wuhan 430074, China

³State Key Laboratory of Optical Communication Technologies and Networks, Wuhan 430074, China

DOI:10.1109/JPHOT.2017.2771221

1943-0655 © 2017 IEEE. Translations and content mining are permitted for academic research only. Personal use is also permitted, but republication/redistribution requires IEEE permission. See http://www.ieee.org/publications_standards/publications/rights/index.html for more information.

Manuscript received October 13, 2017; revised November 2, 2017; accepted November 2, 2017. Date of publication November 8, 2017; date of current version November 17, 2017. This work was supported in part by the National Natural Science Foundation of China under Grants 61431003, 61601049, and 61625104, in part by the National 863 Program under Grant 2015AA016903, and in part by the State Key Laboratory of Advanced Optical Communication System and Networks, Shanghai Jiao Tong University. Corresponding author: J. Li (e-mail: jianqiangli@bupt.edu.cn).

Abstract: We have experimentally demonstrated the signal-to-signal beating interference (SSBI) mitigation capability of Kramers–Kronig (KK) detection in a single sideband (SSB) four-ary pulse-amplitude-modulation (PAM4) direct detection (DD) system. A 112-Gbit/s (56-GBaud) SSB-PAM4 optical signal suitable for KK detection is generated by using a single commercial, low-cost dual-drive Mach–Zehnder modulator. The system bandwidth constraint is mitigated by Nyquist pulse shaping and bandwidth precompensation. The SSBI mitigation capability of KK algorithm is identified by comparing with two order Volterra filter. After 80-km dispersion-uncompensated standard single-mode fiber transmission, linear equalizer with KK algorithm and two order Volterra filter based nonlinearity equalizer show similar bit error rate (BER) performance, which are 3.2×10^{-3} and 2.8×10^{-3} , respectively. Both BERs are below 7% hard-decision forward error correction threshold of 3.8×10^{-3} . The experiment results present the excellent SSBI mitigation capability of KK detection in SSB-PAM4 DD system. Above all, our experiments reveal the potential of KK detection in DD system for data center interconnects.

Index Terms: Beating interference mitigation, direct detection, Kramers–Kronig detection, optical interconnects, pulse amplitude modulation (PAM).

1. Introduction

The evolution from mega data centers to inter-connected clusters of smaller data centers requires high speed and high capacity data center interconnects (DCIs) over up to 80 km. Single-lane 100-Gbit/s and beyond systems with low cost and low power consumption are under intensive research. Due to low cost and simple configuration, the intensity modulation and direct-detection

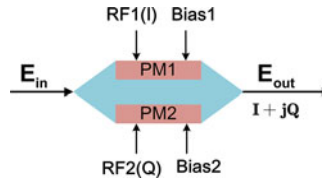


Fig. 1. The principle of SSB optical signal generation by dual-drive MZM (DD-MZM). RF, radio frequency; PM, phase modulator.

(IM/DD) systems are very promising for the inter-DCI applications. To support 100-Gbit/s transmission over up to 80-km SSMF in IM/DD systems, advanced modulation formats are required, such as pulse amplitude modulation (PAM), carrierless amplitude and phase modulation (CAP), discrete multi-tone (DMT), and Nyquist sub-carrier modulation (N-SCM) [1]. Among the candidates above, PAM is preferred and four-ary PAM (PAM4) has been standardized as a modulation scheme for the 400GE standard [1].

However, there are two main constraint factors for high speed PAM4 transmission including the bandwidth limitation of low cost electro-optical components and the distortion induced by chromatic dispersion (CD). The constraint of system bandwidth can be mitigated by using Nyquist pulse shaping and bandwidth pre-compensation [2]. Besides, cost-effective approaches mitigating the influence of CD have been studied for PAM4 IM/DD systems, such as CD pre-compensation technique [1] and single sideband (SSB) technique [3], [4]. The SSB technique is more suitable than CD pre-compensation technique for flexible deployment of both single-lane and wavelength division multiplexed (WDM) systems since the knowledge of the total dispersion is not necessary at the transmitter. Nevertheless, signal to signal beating interference (SSBI) generated by square-law detection and aggravated by accumulated CD in fiber transmission will deteriorate the system performance in a SSB-PAM4 DD system. Many digital compensation techniques have been proposed to mitigate the influence of SSBI, such as receiver-based estimation and cancellation technique [5] and two order Volterra filter (VF) [4], [6]. Recently, a more effective SSBI mitigation scheme, which is based upon Kramers-Kronig (KK) coherent receiver [7], has been utilized to mitigate the SSBI in DMT DD system [8] and Nyquist-SCM DD system [5]. This KK detection-based scheme shows predominant SSBI mitigation capability. Compared with the SSBI mitigation schemes mentioned above, KK scheme has the advantages of receiver-side digital CD compensation and lower DSP complexity since it makes the optical DD channel a linear and complex channel similar to a coherent system. The reduction in computation complexity indicates KK scheme's potential in fast-growing DCI applications, which requires low cost and low power consumption. Although the receiver-side digital CD compensation using KK detection in PAM transmission have been studied by simulations [9], there is no experiments to verify KK detection's effectiveness of SSBI mitigation in PAM4 transmission, to the best of our knowledge. In this paper, we experimentally generate an optical SSB-PAM4 signal suitable for KK detection by using a single commercial, low-cost DD-MZM. The SSBI mitigation capability of KK detection is identified by comparing the performance of KK algorithm plus linear equalizer with the performance of two order Volterra filter-based non-linearity equalizer. By using bandwidth pre-compensation and KK detection, 56-GBaud SSB-PAM4 signal transmission over 80-km dispersion-uncompensated SSMF is achieved with 20 GHz 10-dB bandwidth.

2. Principle of Operation

2.1 Scheme of SSB Complex Modulation

The structure of a typical DD-MZM comprising of two parallel phase modulator (PM) is shown in Fig. 1 and its transfer function is described as [10]:

$$E_{out} = \frac{\sqrt{2}}{2} E_{in} \left(e^{j\frac{\pi}{V_{\pi}} V_1} + e^{j\frac{\pi}{V_{\pi}} V_2} \right) \quad (1)$$

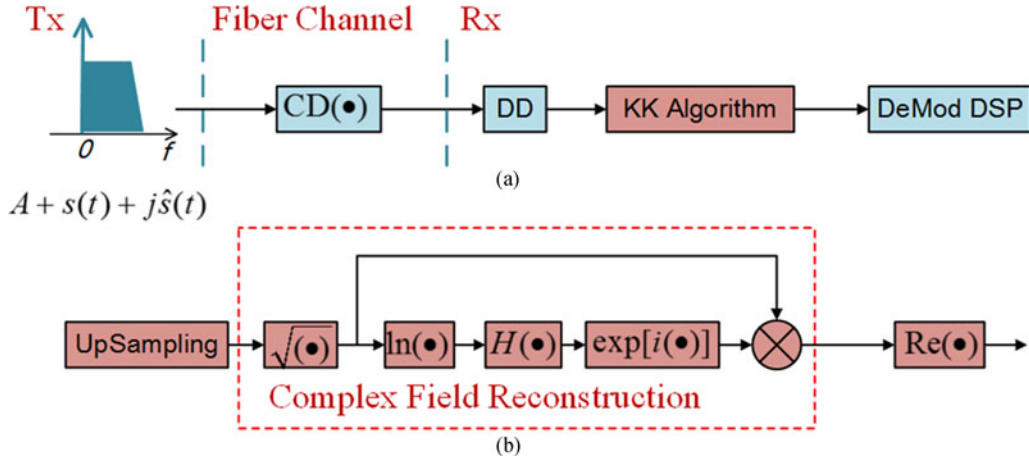


Fig. 2. Transmission scheme using Kramers-Kronig (KK) detection for SSB-PAM4 direct detection (DD) system: (a) SSB-PAM4 DD system diagram; (b) DSP flow of KK algorithm. A is a real constant. $s(t)$ denotes a real PAM4 signal and $\hat{s}(t)$ denotes a Hilbert transform of $s(t)$.

where V_1 and V_2 are the driving voltage signals in each branches, and V_π is the voltage needed to produce a π phase shift in each branch. Both V_1 and V_2 have two components: the bias voltages and the radio frequency (RF) voltage signals carrying information. We replace V_1 and V_2 with $I + \text{Bias}1$ and $Q + \text{Bias}2$, respectively. When $\text{Bias}1 = -V_\pi/2$ and $\text{Bias}2 = 0$, the output of DD-MZM can be expressed as:

$$E_{out} = \frac{\sqrt{2}}{2} E_{in} \left(-je^{j\frac{\pi}{V_\pi}I} + e^{j\frac{\pi}{V_\pi}Q} \right) \quad (2)$$

Considering the 1st-order approximation of $e^x \approx 1 + x$ for small driving signals, (2) changes into

$$E_{out} \approx \frac{\sqrt{2}}{2} E_{in} \left[-j \left(1 + j\frac{\pi}{V_\pi}I \right) + 1 + j\frac{\pi}{V_\pi}Q \right] = \frac{\sqrt{2}}{2} E_{in} \left[1 - j + \frac{\pi}{V_\pi}(I + jQ) \right] \quad (3)$$

As expressed in (3), a complex signal $C = I + jQ$ can be linearly converted to optical domain by a DD-MZM when the RF driving signals are small. Naturally, we can generate a SSB-PAM4 optical signal by driving the DD-MZM with a PAM4 real signal $s(t)$ and its Hilbert transform $\hat{s}(t)$. However, the peak average power ratio (PAPR) of $\hat{s}(t)$ is much higher than $s(t)$ and it might bring imbalanced impairments for I and Q paths if we directly apply $s(t)$ and $\hat{s}(t)$ on the DD-MZM. Besides, the obtained SSB signal given by $\pi(s(t) + j\hat{s}(t))/V_\pi$ is not aligned with the carrier given by $(1-j)$ and thus the condition of minimum phase is not satisfied [7], [8]. To solve these two problem, the driving signals I and Q are set as depicted in (4) and (5) [10]:

$$I(t) = \hat{s}(t) + s(t) \quad (4)$$

$$Q(t) = \hat{s}(t) - s(t) \quad (5)$$

By this means, the SSB-PAM4 optical signal suitable for KK detection is generated and it can be written as:

$$E_{out} \approx \frac{\sqrt{2}}{2} (1 - j) E_{in} \left[1 + \frac{\pi}{V_\pi} (s(t) + j\hat{s}(t)) \right] \quad (6)$$

2.2 SSB-PAM4 Transmission Scheme Using Kramers-Kronig Detection

The transmission scheme based on KK detection is illustrated in Fig. 2. For a SSB-PAM4 optical signal given by $A + s(t) + j\hat{s}(t)$, where A denotes a real constant, it is a minimum phase signal when

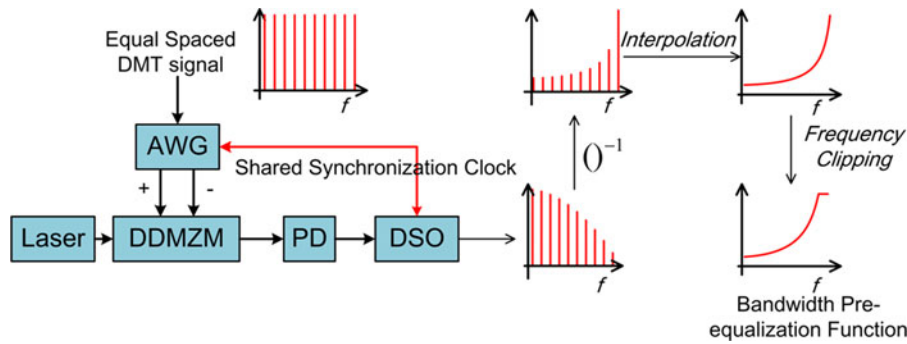


Fig. 3. The approach to get a bandwidth pre-compensation function of the system. DMT: discrete multitone; AWG: arbitrary waveform generator; PD, photo detector; DSO, digital sampling oscilloscope.

$|A| > |s(t) + j\hat{s}(t)|$. So this optical signal's phase is linked to its intensity based on KK relations [7], [8]. Hence, the complex field imping upon the photo detector (PD) can be reconstructed through KK relations as expressed in (7) and (8):

$$\phi_E(t) = H[1n(\sqrt{I_{opt}})] \quad (7)$$

$$E(t) = \sqrt{I_{opt}(t)} \exp(j\phi_E(t)) \quad (8)$$

where $I_{opt}(t)$ and $\phi_E(t)$ denote the intensity measured by the PD and the phase of the complex field, respectively, and $H[\cdot]$ is a Hilbert transform operator. It should be noted that up-sampling is needed before complex field reconstruction (CFR) due to the high bandwidth resulting from the square-root and logarithm operations [5], [7]. Digital up-sampling by a factor of 3 is sufficient for the following CFR [7]. Following CFR, SSBI-mitigated PAM4 signal is obtained by taking the real part of the complex signal.

2.3 Bandwidth Precompensation

In our experiment, the bandwidth pre-compensation is enabled by off-line measurement of channel amplitude response. Thus we can calculate the inverse of channel amplitude response, which is used to generate a finite impulse response (FIR) filter for pre-compensation. As depicted in Fig. 3, the arbitrary waveform generator (AWG) shares the same synchronization clock with the digital sampling oscilloscope (DSO) to realize a synchronization between the transmitter and the receiver [1]. An equal spaced DMT signal is then fed to a DD-MZM in a differential way. The envelope of the received signal's amplitude response is the channel amplitude response. Finally, the inverse of the amplitude response is calculated to generate the bandwidth pre-equalization function and the bandwidth pre-compensation is enabled.

3. Experimental Setup

As shown in Fig. 4, the experiment is conducted as follows. At the transmitter side, quaternary PRBS13 test pattern according with 400GE standard is first mapped to PAM4 symbols and the generated 56-GBaud PAM4 symbols are then up-sampled by a factor of 4 for pulse shaping. A square-root-raised-cosine pulse shape with a roll-off factor of 0.15 is used to reduce the signal bandwidth to 32.2 GHz, and bandwidth pre-compensation is adopted to further mitigate the bandwidth limitation by using a digital FIR filter. Following pulse shaping and bandwidth pre-compensation, the signal is then resampled to 64 GSa/s and a Hilbert transform operator is carried out. The RF driving signals, I and Q , are generated in the way of $I = \hat{s}(t) - s(t)$ and $Q = \hat{s}(t) + s(t)$ by using Keysight M8195A AWG with 20 GHz 3-dB bandwidth. The driving signals are then fed to a 30-GHz DDMZM (FTM7937EZ from Fujitsu) biased at its quadrature point to get a SSB optical signal. The

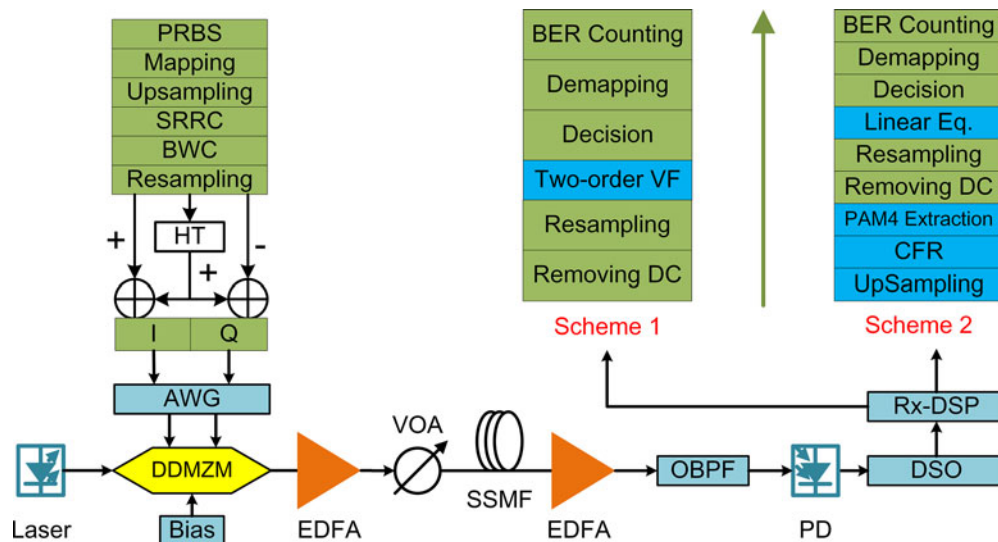


Fig. 4. Experimental setup and offline DSP flow. SRRC, square root raised cosine; BWC, bandwidth pre-compensation; HT, Hilbert transform; DSP, digital signal processing; EDFA, erbium-doped fiber amplifier; VOA, variable optical attenuator; OBPF, optical band pass filter; DSO, digital sampling oscilloscope; CFR, complex field reconstruction; Linear Eq., linear equalization; VF, Volterra filter.

voltage to produce a π phase shift in each branch for this DDMZM is round 3.5 V according to the specifications. At the receiver side, the optical signals are detected by a 30-GHz dc coupling PIN PD (XPDV2120R from Finisar). The electrical signal from the PD is digitized and captured with 2 million samples in each case by a 160-GSa/s Lecroy digital sampling oscilloscope (DSO) (Lab-Master 10-59Zi-A) with 59-GHz 3-dB bandwidth for offline processing. Finally, two DSP schemes are investigated. Both the two schemes are aimed to mitigate the influence of SSBI resulting from direct detection. Scheme 1 utilizes two order Volterra filter-based nonlinear equalizer while Scheme 2 adopts linear equalizer with KK algorithm. The linear and nonlinear equalizer are both based upon the cascade of the standard least-mean-square (LMS) algorithm with training sequence and conventional decision-directed-least-mean-square (DD-LMS) algorithm. After equalization, the bit error rate (BER) is calculated following symbol decision and Gray-demapping.

4. Experimental Results and Discussion

As depicted in Fig. 5(a), the system 3-dB bandwidth is round 7 GHz. This strong bandwidth constraint is a result of the cascade filtering of electric and optical components. Fortunately, the 10-dB bandwidth of the system reaches 20 GHz which makes 112-Gb/s PAM4 possible. A sideband suppression ratio of 22 dB is obtained after modulation as depicted in Fig. 5(b). This indicates the good effect of the DD-MZM-based SSB modulation scheme. In our experiments, we first test the system performance in B2B case. For DSP Scheme 1 and DSP Scheme 2, the system performances are compared and BER curves obtained are shown in Fig. 6. The memory length for two order VF is (61, 21), after optimization while the number of FIR filter taps for linear equalizer in Scheme 2 is also set as 61 for fair comparison. To verify the benefit of bandwidth pre-compensation, the performances without and with bandwidth pre-compensation for both two DSP schemes are compared. One can see that bandwidth pre-compensation brings a great improvement on BER performance for both Scheme 1 and Scheme 2. As shown in Fig. 6(a), a floor appears at 900 mV when using bandwidth pre-compensation since relative small signal is needed for our SSB modulation scheme. The driving signal amplitude and the received optical power for fiber transmission are chosen to be 1000 mV and 7 dBm, respectively. Unexpectedly, one can see that Scheme 1 has a better

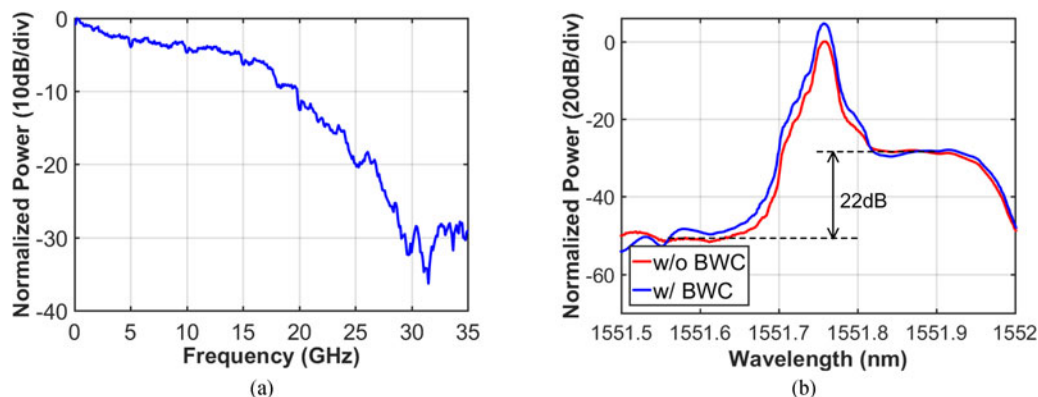


Fig. 5. (a) Measured system transfer function; (b) optical spectrums of the modulated SSB signal without and with bandwidth pre-compensation.

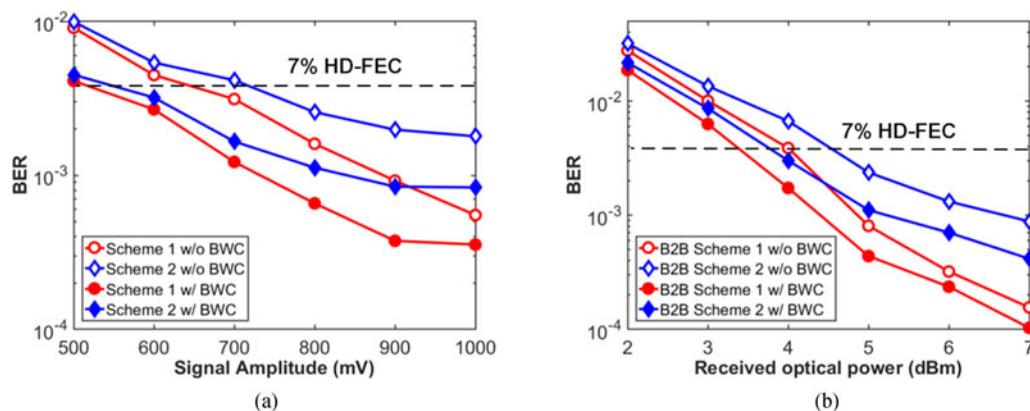


Fig. 6. BER performance comparison in B2B case: (a) BER as a function of driving signal amplitude without BWC and with BWC; (b) BER as a function of received optical power without BWC and with BWC. HD-FEC, hard decision forward error correction.

performance than Scheme 2 in B2B case when the driving signal amplitude and the received optical power increase. Simulations are made to find the reason for this phenomena. The V_{π} of the DDMZM is set as 3 V in the simulations. To analyze the influence of bandwidth limitations and carrier to signal power ratio (CSPR), BER performance over different driving signal amplitude with 22 GHz 3-dB bandwidth and 42 GHz 3-dB bandwidth are plotted in Fig. 7(a) and (b), respectively. When the system 3-dB bandwidth increases from 22 GHz to 42 GHz, an improvement on BER performance is observed for both Scheme 1 and Scheme 2. However, the performance of Scheme 2 is still inferior to the performance of Scheme 1 even with 3-dB bandwidth of 42 GHz. So the bandwidth limitation is not the main reason for the difference between Scheme 1 and Scheme 2. On the other hand, the driving signal amplitude has a greater impact on performance as shown in Fig. 7. With the increase of signal amplitude, system's signal to noise ratio (SNR) increase at the same time, which improves the performance. But CSPR decreases during the increase of signal amplitude. If CSPR is not enough to meet with the requirement of minimum phase, CFR will be affected for KK algorithm. Hence, the performance of Scheme 2 will be limited by imperfect reconstruction when the signal amplitude increases as shown in Figs. 6(a) and 7.

Further, we carry out fiber transmission experiments. To get the optimal system performance, different launched optical power is tested and the results are shown in Fig. 8(a). As depicted in Fig. 8(a), the optimal launched optical power is round 9 dBm and we choose it for our fiber

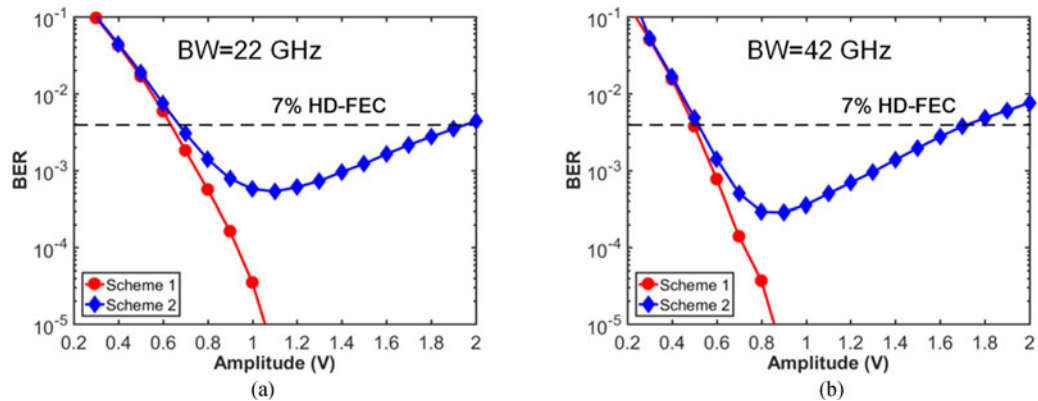


Fig. 7. The simulation analysis on BER over different driving signal amplitude in B2B case: (a) with a system 3-dB bandwidth of 22 GHz; (b) with a system 3-dB bandwidth of 42 GHz. BW, bandwidth.

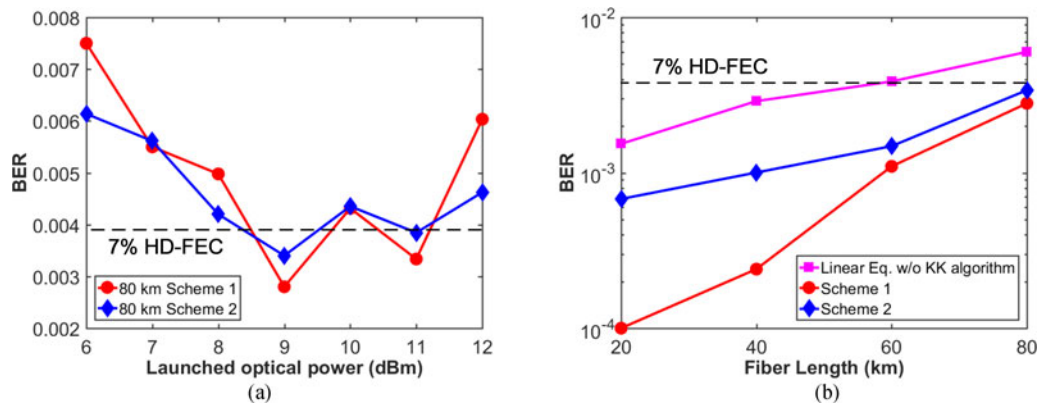


Fig. 8. (a) BER as a function of launched power in fiber transmission experiments. (b) BER as a function of fiber length in fiber transmission experiments.

transmission experiments. Next, BER performance with different fiber lengths are measured. To verify the SSBI mitigation effects of two order VF and KK algorithm, linear equalizer without KK algorithm are used to be a contrast for both Scheme 1 and Scheme 2. Considering the pulse spreading induced by CD, the number of FIR taps of linear equalizer is increased to 91 and the memory length of two order VF is increased to (91, 25). As shown in Fig. 8(b), one can see that both the two schemes have a good improvement relative to linear equalizer without KK algorithm. Similar to B2B case, Scheme 1 exceeds Scheme 2 greatly for 20-km and 40-km SSMF transmission due to affected CFR. However, when fiber length increased to 60 km and 80 km, two order VF and linear equalizer with KK algorithm present the similar performance. We make simulations on fiber transmission to study the phenomena. The optical signal to noise ratio (OSNR) keeps the same for different fiber length. For different fiber lengths, BERs over different driving signal amplitude with 22 GHz 3-dB bandwidth and 42 GHz 3-dB bandwidth are plotted in Figs. 9 and 10. Even though the OSNR is the same over different fiber length, the performance of Scheme 1 degrades severely as the fiber length increases. It shows that dispersion limits the SSBI mitigation capability of two order VF. However, the performance of Scheme 2 almost remains the same over varying fiber length and it indicates the good tolerance of KK algorithm to CD.

For two order VF-based nonlinear equalizer and linear equalizer with KK algorithm, BERs after 80-km SSMF transmission are 2.8×10^{-3} and 3.2×10^{-3} , respectively. Both BERs are below the 7% hard-decision forward error correction threshold of 3.8×10^{-3} . Nevertheless, it should be

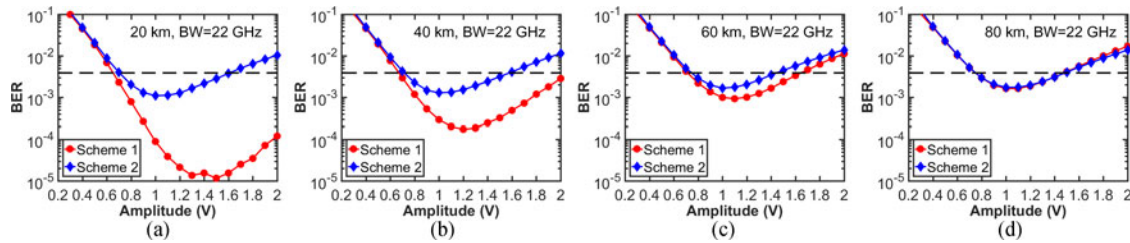


Fig. 9. The simulation analysis on BER over different driving signal amplitude in fiber transmission case with system 3-dB bandwidth of 22 GHz: (a) 20 km; (b) 40 km; (c) 60 km; (d) 80 km.

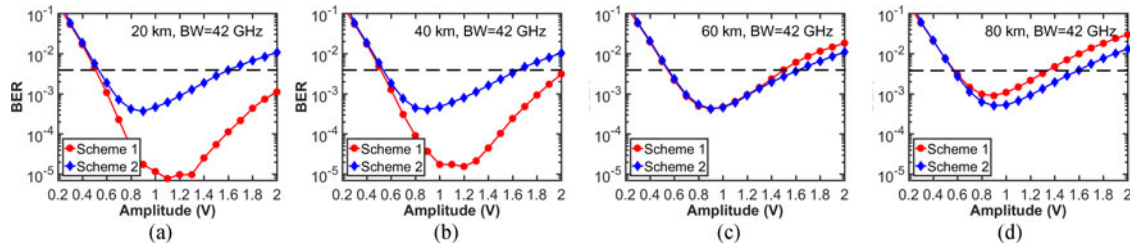


Fig. 10. The simulation analysis on BER over different driving signal amplitude in fiber transmission case with system 3-dB bandwidth of 42 GHz: (a) 20 km; (b) 40 km; (c) 60 km; (d) 80 km.

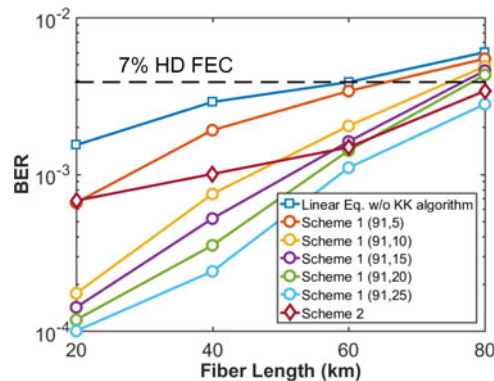


Fig. 11. The optimization for two order memory length of Volterra filter.

noted that Scheme 1 has much lower computation complexity than Scheme 2 at a fiber length of 80 km. We define the computation complexity as the number of multiplications in an algorithm [11]. For two order VF with a memory length of (L_1, L_2) , the number of 1st-order kernels and 2nd-order kernels are L_1 and $(L_2 \times (L_2 + 1))/2$ [12], respectively. To avoid the high computation complexity of two order Volterra filter caused by the large two order memory length, different two order memory length is tested to find the optimal value. The results are plotted in Fig. 11. Although a two order memory length of 5 is sufficient for 20-km, 40-km and even 60-km fiber transmission, two order memory length of 25 and beyond is still needed for 80-km fiber transmission. The two order VF with a memory length of (91, 25) has 91 1st-order kernels and 325 2nd-order kernels. The computation complexity of the two order VF-based nonlinear equalizer is $91 + 2 \times 325 = 741$ while the computation complexity of the linear equalizer is 91. Hence, the equalizer reduces 87% computation complexity by using KK algorithm. Since the computation complexity of the square-root operation, logarithm operation and Hilbert transform included in KK algorithm is relatively low, Scheme 1 has much lower computation complexity than Scheme 2.

5. Conclusion

In summary, 56-GBaud SSB-PAM4 transmission over 80-km dispersion-uncompensated SSMF is demonstrated by using low-complexity linear equalizer with KK algorithm. The experiment results present that the linear equalizer with KK algorithm has the similar SSBI mitigation ability to two order VF when reducing much computation complexity. Above all, this experiment reveals the potential of KK detection in DD system again.

References

- [1] Q. Zhang, N. Stojanovic, C. Xie, C. Prodaniuc, and P. Laskowski, "Transmission of single lane 128 Gbit/s PAM-4 signals over an 80 km SSMF link, enabled by DDMZM aided dispersion pre-compensation," *Opt. Exp.*, vol. 24, no. 21, pp. 24580–24591, Oct. 2016.
- [2] Q. Zhang, N. Stojanovic, C. Prodaniuc, C. Xie, M. Koenigsmann, and P. Laskowski, "Single-lane 180 Gbit/s PAM-4 signal transmission over 2 km SSMF for short-reach applications," *Opt. Lett.*, vol. 41, no. 19, pp. 4449–4452, Oct. 2016.
- [3] N. Kaneda, J. Lee, and Y.-K. Chen, "Nonlinear equalizer for 112-Gb/s SSB-PAM4 in 80-km dispersion uncompensated link," in *Proc. Int. Conf. Opt. Fiber Commun.*, 2017, Paper Tu2D.5.
- [4] M. Zhu *et al.*, "Hilbert superposition and modified signal-to-signal beating interference cancellation for single side-band optical NPAM-4 direct-detection system," *Opt. Exp.*, vol. 25, no. 11, pp. 12622–12631, May 2017.
- [5] Z. Li *et al.*, "SSBI mitigation and the kramers–kronig scheme in single-sideband direct-detection transmission with receiver-based electronic dispersion compensation," *J. Lightw. Technol.*, vol. 35, no. 10, pp. 1887–1893, May 2017.
- [6] X. Li *et al.*, "Transmission of 4×28 -Gb/s PAM-4 over 160-km single mode fiber using 10G-Class DML and photodiode," in *Proc. Int. Conf. Opt. Fiber Commun.*, 2016, Paper W1A.5.
- [7] A. Mecozzi, C. Antonelli, and M. Shtaif, "Kramers–Kronig coherent receiver," *Optica*, vol. 3, no. 11, pp. 1220–1227, Nov. 2016.
- [8] C. Antonelli, A. Mecozzi, and M. Shtaif, "Kramers-Kronig PAM Transceiver," in *Proc. Int. Conf. Opt. Fiber Commun.*, 2017, Paper Tu3I.5.
- [9] X. Chen *et al.*, "218-Gb/s single-wavelength, single-polarization, single-photodiode transmission over 125-km of standard singlemode fiber using kramers-kronig detection," in *Proc. Int. Conf. Opt. Fiber Commun.*, 2017, Paper Th5B.6.
- [10] Q. Zhang *et al.*, "Demonstration of CD pre-compensated direct detection PAM4 40 km transmission in C-band using DDMZM," in *Proc. Int. Conf. Asia Commun. Photon.*, 2016, Paper ATH3C.2.
- [11] S. Zhou, X. Li, L. Yi, Q. Yang, and S. Fu, "Transmission of 2×56 Gb/s PAM-4 signal over 100 km SSMF using 18 GHz DMLs," *Opt. Lett.*, vol. 41, no. 8, pp. 1805–1808, Apr. 2016.
- [12] F. Gao *et al.*, " 2×64 Gb/s PAM-4 transmission over 70 km SSMF using O-band 18G-class directly modulated lasers (DMLs)," *Opt. Exp.*, vol. 25, no. 7, pp. 7230–7237, Apr. 2017.